Quaternary Science Reviews 206 (2019) 56–64

Contents lists available at ScienceDirect

Quaternary Science Reviews

journal homepage: www.elsevier.com/locate/quascirev

Anthropogenic effects on tropical oceanic climate change and variability: An insight from the South China Sea over the past 2000 years

Wenfeng Deng [a, b, *], Gangjian Wei [a], Jian-xin Zhao [b], Ti Zeng [c]

[a] State Key Laboratory of Isotope Geochemistry, Guangzhou Institute of Geochemistry, Chinese Academy of Sciences, Guangzhou, 510640, China
[b] Radiogenic Isotope Facility, School of Earth and Environmental Sciences, The University of Queensland, Brisbane, Queensland, 4072, Australia
[c] Key Laboratory of Marginal Sea Geology, Guangzhou Institute of Geochemistry, Chinese Academy of Sciences, Guangzhou, 510640, China

ARTICLE INFO

Article history:
Received 12 January 2018
Received in revised form
27 December 2018
Accepted 28 December 2018
Available online 7 January 2019

Keywords:
Human activity
Anthropogenic CO_2
Oceanic climate change
Oceanic climate variability
Past 2000 years
South China Sea
Coral

ABSTRACT

To better understand the effect of human activities on tropical oceanic climate change, existing coral-based paleoclimate data from the northern South China Sea (SCS) for several representative climate periods over the past 2000 years were synthesized and reanalyzed. The sea surface temperature (SST) during the current warm period (CWP), in which the climate has been influenced by human activities, exhibits larger change amplitude and higher oscillation frequency than during periods in which the climate was controlled by natural forcings. However, the variabilities of the sea water $\delta^{18}O$ ($\delta^{18}O_{sw}$) during the four climate periods over the past 2000 years examined here are somewhat complicated to decipher. The variation amplitudes are variable but the interannual oscillations are similar during different periods. Even so, high variability during the CWP may still suggest the anthropogenic effects on tropical oceanic hydroclimate. This may implies that the anthropogenic effects intensify the tropical SST and hydrological variation both in amplitude and frequency. The decoupling between coral $\delta^{13}C$ and total solar insolation during the CWP may be a result of the oceanic $\delta^{13}C$ Suess effect from the addition of anthropogenic $^{12}CO_2$ to the surface ocean. This suggests that increased anthropogenic CO_2 caused the main carbon source and the utilization process of coral reefs during calcification to change. To accurately assess the influence of human activities on oceanic climate and environmental change, the effects of anthropogenic CO_2 should be monitored continuously over a longer time frame.

© 2018 Elsevier Ltd. All rights reserved.

1. Introduction

The effect of increasing human activities since the beginning of the Industrial Revolution on global climate is a major issue in the scientific community (Kellogg, 1977; Karl and Trenberth, 2003; Oreskes, 2004). The Intergovernmental Panel on Climate Change (IPCC) reported in 2014 "It is extremely likely that more than half of the observed increase in global average surface temperature from 1951 to 2010 was caused by the anthropogenic increase in greenhouse gases concentrations and other anthropogenic forcings together" (IPCC, 2014). Concurrently, anthropogenic CO_2 has been reported to have a significant effect on the land and ocean carbon cycles (Ciais et al., 2013). However, there is still continuous scientific, media, public, and political debate on the effect of anthropogenic global warming since the mid-to late-1980s (Khandekar et al., 2005).

To better assess the effect of human activities on global climate, studying the change in climate over the last two millennia is important (Mann, 2007). The last two millennia are important because they include several key climate periods, such as the Medieval Climate Anomaly (MCA, AD 900–1300) (Lamb, 1965; Crowley and Lowery, 2000), the Little Ice Age (LIA, AD 1550–1850) (Robock, 1979; Bradley and Jones, 1993), and the Current Warm Period (CWP, AD 1850–present) (Wu et al., 2012; Fleury et al., 2015). The MCA and LIA periods occurred before the Industrial Revolution and associated climate anomalies were driven by natural forcing (e.g., solar variability and volcanic emissions). The ongoing CWP includes the Industrial Revolution and is dominated by anthropogenic factors (e.g., industrialization and land-use

* Corresponding author. State Key Laboratory of Isotope Geochemistry, Guangzhou Institute of Geochemistry, Chinese Academy of Sciences, Guangzhou, 510640, China.,
E-mail addresses: wfdeng@gig.ac.cn, w.deng@uq.edu.au (W. Deng).

https://doi.org/10.1016/j.quascirev.2018.12.027
0277-3791/© 2018 Elsevier Ltd. All rights reserved.

changes) (Masson-Delmotte et al., 2013).

Modern instrumental temperature observations cover only the last 150 years, and are clearly insufficient for examining changes that occurred many centuries ago or assessing the anthropogenic effect since the Industrial Revolution. Therefore, historical records are extended with the use of proxy data (Mann, 2002). However, an overwhelming majority of the proxy-based climate reconstruction records for the past two millennia were collected from high latitude terrestrial regions, and records from the tropical oceans are rare (Mann et al., 2008). Further, terrestrial records are not consistent with each other (Mann et al., 2008). The oceans cover over 70% of the Earth's surface and mediate the response of global climate to natural and anthropogenic forcings (McGregor et al., 2015). In addition, the oceans are intrinsically linked to the atmosphere through processes such as the storage and global dispersion of heat, evaporation, freezing and thawing in polar regions, and the storage and exchange of gases, including CO_2 (Herr and Galland, 2009). Therefore, obtaining climate records from the oceans over the past 2000 years could provide an improved quantification of the range of natural climate variability mediated by the ocean, and attribute recent changes to anthropogenic or natural drivers. Massive corals are one of the most reliable sources of proxies used to reconstruct climate and environmental records from the oceans because they incorporate isotope and elemental tracers during skeletal growth that reflect the ambient environmental conditions (Lough, 2010). In addition, massive corals contain distinct annual growth bands and have high growth rates, thereby providing high-resolution and dateable climate information about the surrounding seawater in which they lived (Gagan et al., 2000; Lough, 2010).

The climate in the South China Sea (SCS), which is the largest marginal sea of the western tropical Pacific, is controlled by the East Asian Summer Monsoon (EASM) and the El Niño–Southern Oscillation (ENSO) over seasonal and interannual timescales, respectively (Wang et al., 2004, 2006). Therefore, climate records over the past 2000 years from the SCS can be utilized to obtain better understanding of tropical oceanic climate change and variability and assess anthropogenic effects on tropical oceanic climate. Here, we synthesize and reanalyze existing coral-based paleoclimate data from the northern SCS for several representative climate periods over the past 2000 years to identify differences in climate change and variability before and after the Industrial Revolution and assess anthropogenic effects on tropical oceanic climate change and variability.

2. Materials and methods

The paleoclimate data synthesized here were extracted from six *Porites lutea* colonies in water depths of 4–6 m on fringing reefs off the eastern coast of Hainan Island in the northern SCS. Hainan Island has an oceanic tropical climate that is controlled by the East Asian monsoon. The summer monsoon occurs during May to October and delivers warmer and fresher conditions (e.g., sea surface temperature (SST) of 27–33 °C and sea surface salinity (SSS) of 25–31psu), whereas the winter monsoon dominates during November to April and delivers colder and saltier conditions (e.g., SST of 17–27 °C and SSS of 31–33 psu). The modern coral 11LW4 and the fossil coral 11LW2 were collected at Longwan (11LW4: 19°17′11.94″N, 110°17′11.94″E; 11LW2: 19°17′18.84″N, 110°39′23.40″E) in April 2011. The fossil corals 11QG1 and 11QG3 were collected at Qingge (11QG1: 19°18′30.48″N, 110°40′2.46″E; 11QG3: 19°18′3.72″N, 110°39′41.52″E) also in April 2011. The fossil coral 13OC4 was collected at Oucun (19°19′11.22″N, 110°41′31.26″E) in August 2013. The fossil coral 14FJ12 was collected at Fengjiawan (19°23′43.14″N, 110°45′11.16″E) in July 2014. The sampling locations are shown in Fig. 1 and listed in Table 1. The U–Th dated age, Common Era (CE) growing period, and corresponding representative climate period for each coral is also listed in Table 1. The annually resolved Sr/Ca, $\Delta\delta^{18}O$, $\delta^{13}C$, and $\delta^{11}B$ values, and trace

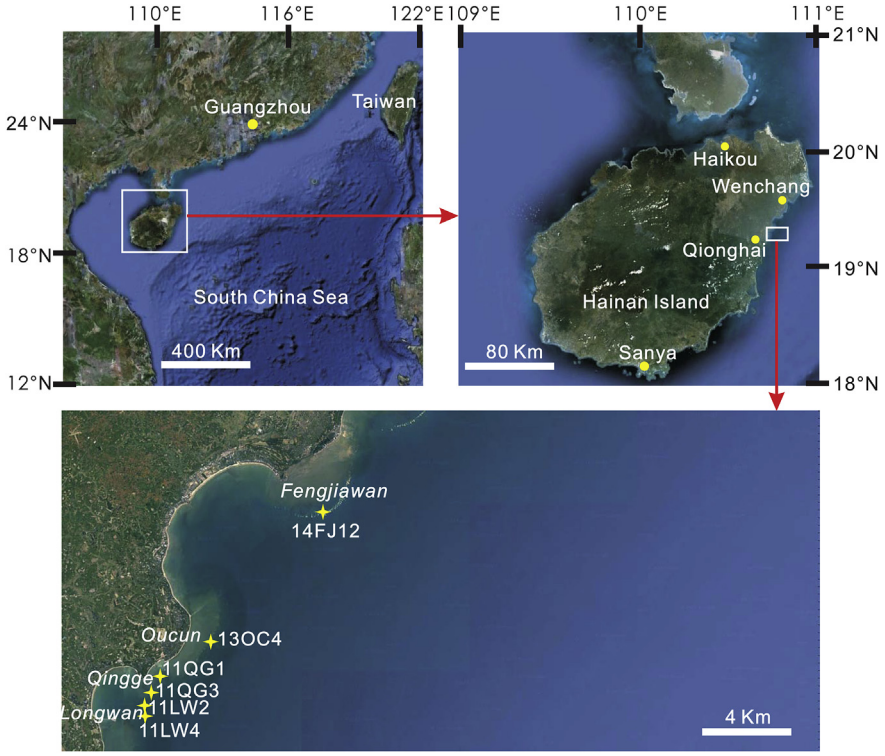

Fig. 1. Satellite images of Hainan Island and the northern SCS. Yellow stars in the lower panel indicate sampling locations. (For interpretation of the references to colour in this figure legend, the reader is referred to the Web version of this article.)

Table 1
Coral samples and corresponding U–Th ages and climate periods.

Coral Name	Location	U-Th Age (±2σ, yr BP)	Growing Period (AD)	Representative Climate Period
11LW4	Longwan (19°17′11.94″N, 110°17′11.94″E)	N/A	1853–2011	Current Warm Period
13OC4	Oucun (19°19′11.22"N, 110°41′31.26"E)	254 ± 4	1702–1772	Little Ice Age
11LW2	Longwan (19°17′18.84"N, 110°39′23.40"E)	371 ± 18	1628–1657	
11QG1	Qingge (19°18′30.48"N, 110°40′2.46"E)	756 ± 10	1129–1255	Medieval Climate Anomaly
11QG3	Qingge (19°18′3.72"N, 110°39′41.52"E)	929 ± 24	1063–1087	
14FJ12	Fengjiawan (19°23′43.14"N, 110°45′11.16"E)	1712 ± 8	167–309	Beginning of CE

metal concentrations of the corals selected for the present study have been previously used to study climate and environmental conditions such as SST, SSS, pH and the oceanic Suess effect of the northern SCS over the past 2000 years (Deng et al., 2013, 2017a; Deng and Wei, 2014; Chen et al., 2015; Wei et al., 2015, 2017b; Xiao et al., 2017). However, the associated changes and variability during the different climate periods are yet to be compared and discussed.

All coral Sr/Ca data were normalized to the value of an international coral standard (JCp-1) prepared by the Geological Survey of Japan (Okai et al., 2002), and then transformed into SST records using the Sr/Ca–SST thermometer, Sr/Ca(mmol/mol) = −0.084 × SST(°C) + 11.278, reported by Gagan et al. (2012). This equation has been corrected for the apparent attenuation effect from the skeletal mass accumulation of coral and can be used to calculate mean SSTs from averaged coral Sr/Ca data, by which the published coral Sr/Ca-SST estimates for the Indo-Pacific region for the last 14,200 years can be recalculated to fall within the 95% confidence of the foraminiferal Mg/Ca-SST records (Gagan et al., 2012).

Coral $\Delta\delta^{18}O$, a proxy for sea water $\delta^{18}O$ ($\delta^{18}O_{sw}$), was calculated by subtracting the SST contribution from the coral $\delta^{18}O$ values (Gagan et al., 1998), according to $\Delta\delta^{18}O = d\delta^{18}O/dT \times [T_{\delta 18O} - T_{Sr/Ca}]$, where $d\delta^{18}O/dT$ is the slope (−0.194‰/°C) of the empirical $\delta^{18}O$–SST function reported by Song et al. (2006), and $T_{\delta 18O}$ and $T_{Sr/Ca}$ are the apparent SSTs calculated from $\delta^{18}O$ values and Sr/Ca ratios, respectively.

To compare the amplitudes of climate change during the different periods, annual SST ($\delta^{18}O_{sw}$) anomalies during each climate period were calculated by centering the SST ($\delta^{18}O_{sw}$) records (subtracting the mean of total data during their respective period from each value).

To extract and compare the climate variability signals during the different periods, spectral analysis was performed on the time series of SST and $\delta^{18}O_{sw}$ using the Paleontological Statistics (PAST) software (Hammer et al., 2001). Prior to spectral analysis, any linear trend in each time series was removed also by the PAST software (Deng and Wei, 2014).

3. Results

Time series of the annual Sr/Ca, $\delta^{18}O$, $\delta^{18}O_{sw}$ and $\delta^{13}C$ during the four representative climate periods examined are presented in Fig. 2. The average annual values of SST reconstructed from the coral Sr/Ca records, and the average annual values of $\delta^{18}O_{sw}$ reconstructed from the coral Sr/Ca records and $\delta^{18}O$ during the different climate periods are listed in Table 2, which was synthesized from Deng et al. (2017b) and Xiao et al. (2017). The average annual SST values are 26.6 °C (1σ = 1.2), 25.1 °C (1σ = 0.8), 26.5 °C (1σ = 0.8), and 25.1 °C (1σ = 0.7) for the CWP, LIA, MCA, and beginning of the CE (BCE), respectively. The difference of the average annual SST values during the MCA and the CWP was not statistically significant at the significance level of 0.05 (Deng et al., 2017b), and so was the situation during the LIA and the BCE ($t = 0.186$, $df = 242$, $p = 0.426$). However, the annual SST value during the LIA was statistically significantly lower than those during the MCA and the CWP (Deng et al., 2017b). The average annual $\delta^{18}O_{sw}$ values are 0.40‰ (1σ = 0.3), 0.12‰ (1σ = 0.2), 0.50‰ (1σ = 0.2), and −0.06‰ (1σ = 0.3) for the CWP, LIA, MCA, and BCE, respectively. The average annual $\delta^{18}O_{sw}$ values during the MCA and the CWP are consistent within the error of coral $\Delta\delta^{18}O$, and they are statistically significantly higher than that during the LIA at the significance level of 0.05 (Deng et al., 2017b). The average annual $\delta^{18}O_{sw}$ values during the BCE was statistically significantly different with those during the other three periods ($t = -18.209$, $df = 293$, $p < 0.00001$ for BCE and MCA; $t = -5.633$, $df = 242$, $p < 0.00001$ for BCE and LIA; $t = -13.432$, $df = 300$, $p < 0.00001$ for BCE and CWP).

The ranges of anomaly amplitudes for SST and $\delta^{18}O_{sw}$ during the different climate periods are shown in Fig. 3 and Fig. 4, respectively, and are also listed in Table 2. The variation amplitudes of SST anomaly were 5.7 °C, 2.9 °C, 3.9 °C, and 2.8 °C for the CWP, LIA, MCA, and BCE, respectively. The variation amplitudes of $\delta^{18}O_{sw}$ anomaly were 1.48‰, 0.85‰, 1.13‰, and 1.49‰ for the CWP, LIA, MCA, and BCE, respectively.

Robust decadal to interdecadal periodicities of approximately 12, 42, and 24 yr at confidence levels of either 90% or 95% in the annual SST records are found during the BCE, MCA, and LIA, respectively (Fig. 3e–g). Interannual periodicities of ~2–7 yr are also significant during these three periods (Fig. 3e–g). For the CWP, only interannual periodicities of ~2–4 yr are robust at confidence levels of either 90% or 95%, and the decadal to interdecadal periodicities are not significant (Fig. 3h). In the annual $\delta^{18}O_{sw}$ records, decadal to interdecadal periodicities of ~12–40 yr and interannual periodicities of ~2–6 yr are robust at confidence levels of either 90% or 95% during all four climate periods (Fig. 4e–h).

4. Discussion

4.1. Change and variability in SST of the northern SCS

A gradual increasing trend is evident in the SST record over the CWP; however, a cooling trend occurred from 1980s onward (Fig. 3d). Although our study sites are exactly located in the areas affected by the summer upwelling system along the northeast coasts of Hainan Island (Jing et al., 2009) and the deep ocean water with an unusual Sr/Ca ratio may lead to an artifact in the Sr/Ca-SST calibration (de Villiers et al., 1994), the coral Sr/Ca can record the SST and the colder conditions related with the intensified summer upwelling during 1930–1960 well (Liu et al., 2013). Therefore, the cooling trend from 1980s may be associated with the intensified summer upwelling. It has been suggested that coastal upwelling areas might show a cooling trend at periods of intense anthropogenic warming of the adjacent land surface (McGregor et al., 2015; Abram et al., 2016). The reason for the enhanced upwelling is the intensification of land-ocean thermal contrasts that drive the upwelling (McGregor et al., 2007).

The long-term average annual SST during both the CWP and MCA are similar (Table 2). The small difference in SST between the CWP and MCA in the northern SCS is similar to that for SSTs of the

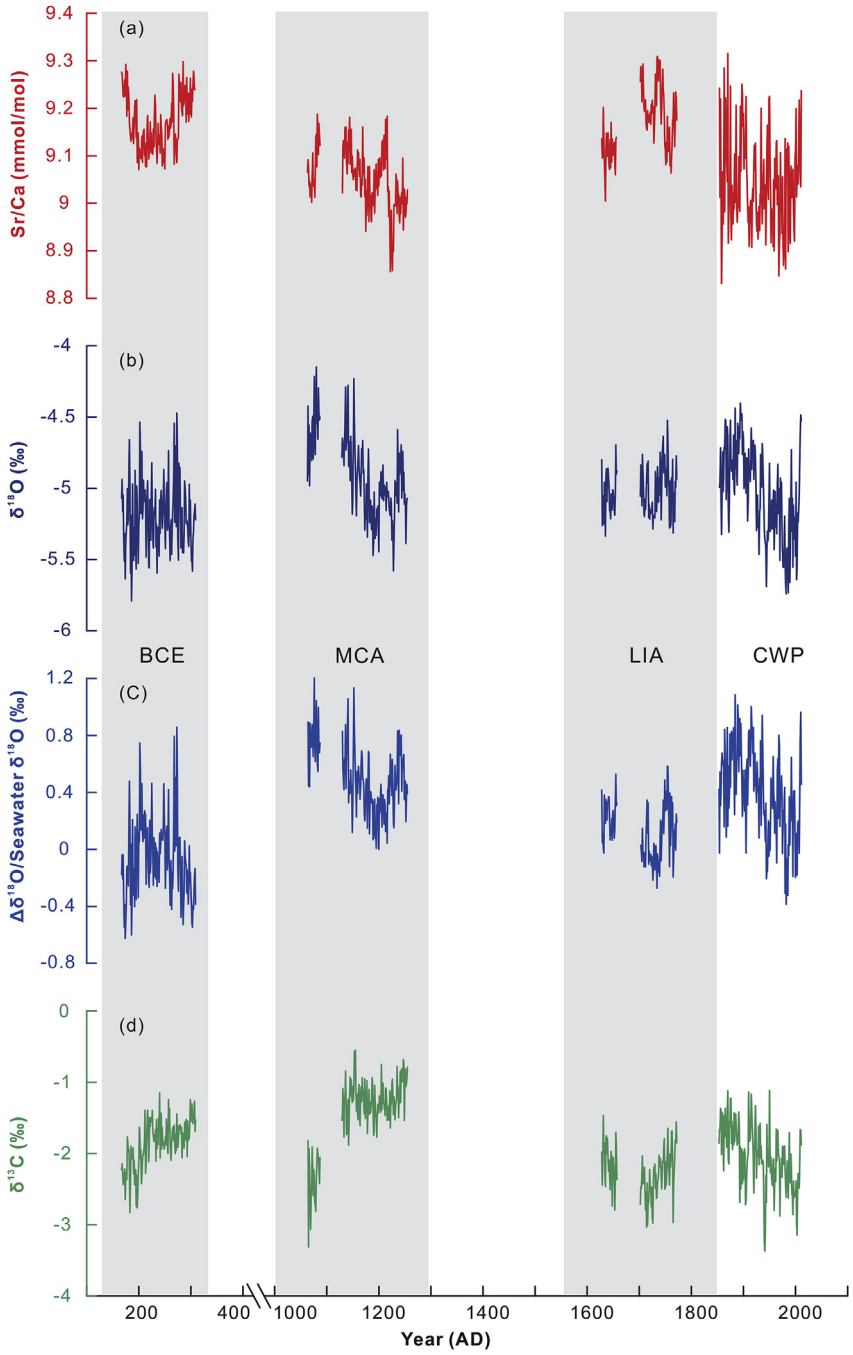

Fig. 2. Time series of (a) coral Sr/Ca, (b) coral $\delta^{18}O$, (c) $\delta^{18}O_{sw}$ reconstructed from paired coral Sr/Ca and $\delta^{18}O$ and (d) coral $\delta^{13}C$ during the BCE, MCA, LIA, and CWP. The gray shading delineates the different periods.

Table 2
SST and $\delta^{18}O_{sw}$ changes during the different climate periods.

Representative Climate Period	Average Annual SST (±1σ, °C)	Variation Amplitude of SST Anomaly (°C)	Average Annual $\delta^{18}O_{sw}$ (±1σ, ‰)	Variation Amplitude of $\delta^{18}O_{sw}$ Anomaly (‰)
Current Warm Period	26.6 ± 1.2	5.7	0.40 ± 0.32	1.48
Little Ice Age	25.1 ± 0.8	2.9	0.12 ± 0.18	0.85
Medieval Climate Anomaly	26.5 ± 0.8	3.9	0.50 ± 0.22	1.13
Beginning of CE	25.1 ± 0.7	2.8	−0.06 ± 0.28	1.49

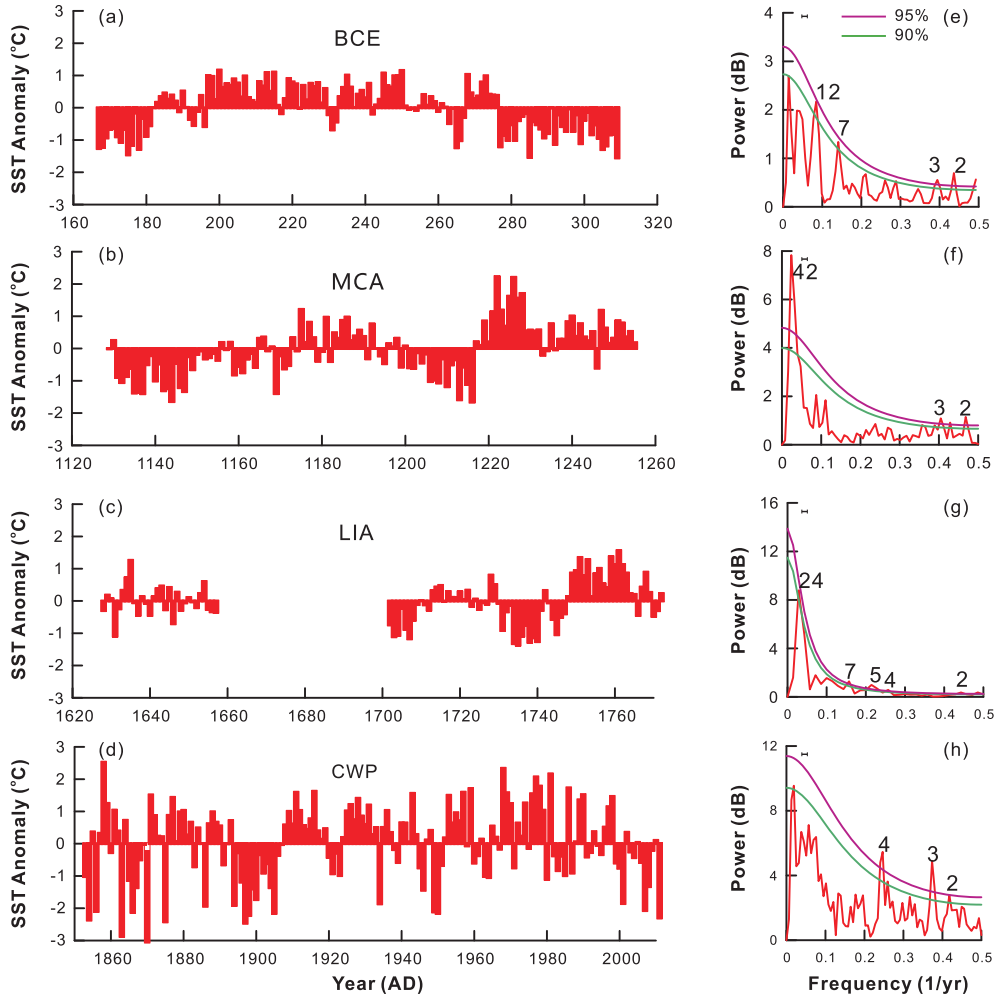

Fig. 3. The anomalies (left panels) and variability (right panels) of SST during the different climate periods of BCE (a and e), MCA (b and f), LIA (c and g), and CWP (d and h). The horizontal bars in the right panels indicate the bandwidths. The purple and green lines indicate the 95% and 90% confidence levels, respectively. (For interpretation of the references to colour in this figure legend, the reader is referred to the Web version of this article.)

Makassar Strait in Indonesia, within the tropical Indo-Pacific warm pool (Oppo et al., 2009). The SST records reconstructed from foraminiferal Mg/Ca records (Fig. 5a) show that the SSTs in the Makassar Strait during the CWP and MCA are comparable given the error range (Oppo et al., 2009). Recent SST records based on long-chain alkenones (Fig. 5b) imply that the MCA was slightly warmer than the CWP in the northern SCS (Kong et al., 2017). In addition, synthesized reconstructions based on terrestrial and marine proxies also suggest that warm anomalies in China during the CWP may not be unprecedented from the last 2000 years, and that the MCA is comparable to the CWP (Ge et al., 2017). Therefore, increased anthropogenic greenhouse gases have led to warming during the CWP in the northern SCS and the tropical Indo-Pacific warm pool, but the level of warming associated with human activities may be not stronger, and even weaker, than that driven by natural climate forcing, such as the increased solar radiation that occurred during the MCA. However, it still should be noted that the SST record reconstructed from a *Tridacna gigas* Sr/Ca profile by Yan et al. (2015a) suggested that the annual average SST was approximately 0.89 °C higher during the MCA than that of the CWP (Fig. 5c). Another record based on the Sr/Ca in a modern coral very close to our sampling site has the average annual SST value of 24.9 °C for the CWP (Liu et al., 2013), which is 1.7 °C lower than our record (Fig. 5c). Although these two coral records were obtained based on different coral standard reference materials and different Sr/Ca-SST relationships, previous studies have demonstrated that coral Sr/Ca differs between adjacent colonies living in the same reef due to vital effects or precipitation efficiency specific to each coral colony (e.g., Pfeiffer et al., 2009; Alpert et al., 2016; Zinke et al., 2016). The uncertainty of the mean annual Sr/Ca-SST estimated from individual fossil eastern Indian Ocean coral colonies has an average of 1.61 °C and can be as large as 2.55 °C (Abram et al., 2009). Therefore, it should be cautious to claim that the MCA and CWP were of similar warmth based on current data.

The warming level observed in SST records during the CWP is not unprecedented compared with the past 2000 years, but the amplitude in the SST variations is much larger than those during the BCE, MCA, and LIA assuming the SST uncertainty of 1.61 °C suggested by Abram et al. (2009) is applicable here. During the three earlier periods, the range of interannual SST anomaly amplitudes are relatively stable, from 2.8 °C during the BCE up to 3.9 °C during the MCA; however, the range increases to 5.7 °C during the CWP (Fig. 3 and Table 2).

In terms of periodicity in the SST variability, both decadal–interdecadal and interannual periodicities are significant during the BCE, MCA, and LIA (Fig. 3e–g). However, the decadal–interdecadal periodicities weaken and only 2–4 yr interannual periodicities are found during the CWP (Fig. 3h). The

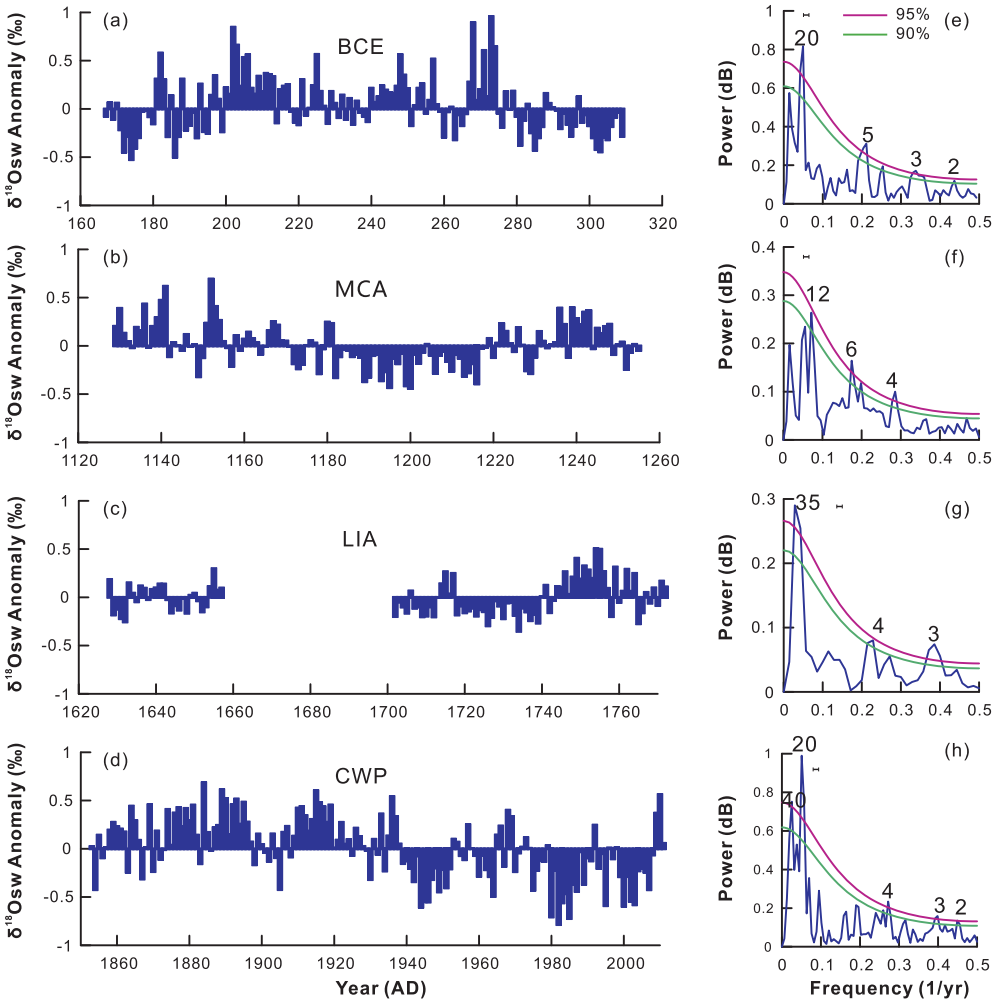

Fig. 4. The anomalies (left panels) and variability (right panels) of $\delta^{18}O_{sw}$ during the different climate periods of BCE (a and e), MCA (b and f), LIA (c and g), and CWP (d and h). The horizontal bars in the right panels indicate the bandwidths. The purple and green lines indicate the 95% and 90% confidence levels, respectively. (For interpretation of the references to colour in this figure legend, the reader is referred to the Web version of this article.)

decadal–interdecadal and interannual periodicities are potentially associated with the Pacific Decadal Oscillation (PDO) and ENSO, respectively (Wang et al., 2006; Deng et al., 2013). However, the attenuation of low frequency variability and strengthening of high frequency variability is presumably a result of the intensification in human activities during the CWP.

Therefore, a larger variation range and higher frequency variability in the SST records during the CWP may suggest that anthropogenic effects intensify western tropical Pacific SST variability both in amplitude and frequency, compared with periods driven by natural forcings. Similar increase in the strength and frequency of tropical climate variability during the twentieth century in the Indian Ocean has also been documented by coral $\delta^{18}O$ records, which may be associated with anthropogenic greenhouse warming (Abram et al., 2008).

4.2. Change and variability in $\delta^{18}O_{sw}$ of the northern SCS

Long-term trends in $\delta^{18}O_{sw}$ variation in the northern SCS during the four climate periods roughly agree with those of several hydroclimate indices (Fig. 6) reconstructed from foraminiferal and stalagmite geochemical proxies in the western Pacific (Oppo et al., 2009; Griffiths et al., 2016). Consistency of the hydrological conditions between the northern SCS and western Pacific indicates that the $\delta^{18}O_{sw}$ in the SCS may be affected by the larger regional hydroclimate over the past 2000 years. The large discrepancy between the coral and stalagmite records during the LIA may result from the increase in rainfall in the northern SCS, which may have been caused by the retreat of East Asian Summer Monsoon during that period (Yan et al., 2015b).

The long-term average annual $\delta^{18}O_{sw}$ values during the CWP and MCA are more positive than those during the LIA and BCE (Table 2). If the $\delta^{18}O_{sw}$ error of 0.25‰ obtained by Nurhati et al. (2011) is applied here, the variation amplitudes in interannual $\delta^{18}O_{sw}$ during the CWP and the BCE (1.48‰ and 1.49‰, respectively) are comparable and exhibit no distinct difference, which are much higher than that during the MCA (1.13‰) (Fig. 4 and Table 2). The situation during the LIA is definitely different from other periods, during which the variation amplitude in $\delta^{18}O_{sw}$ is lowest (Fig. 4 and Table 2). Between AD 1160 and AD 1255 also the MCA shows very low $\delta^{18}O_{sw}$ variation amplitude (Fig. 4b).

In terms of periodicity in the $\delta^{18}O_{sw}$ variability, both decadal–interdecadal and interannual periodicities are significant during all climate periods except the LIA (Fig. 4e–h). The 35 yr interdecadal periodicity is questionable since the record during LIA lasts only 70 years. Similar decadal–interdecadal variability to that observed in the $\delta^{18}O_{sw}$ in the SCS was also found in the main hydrological signal time series reconstructed from stalagmite

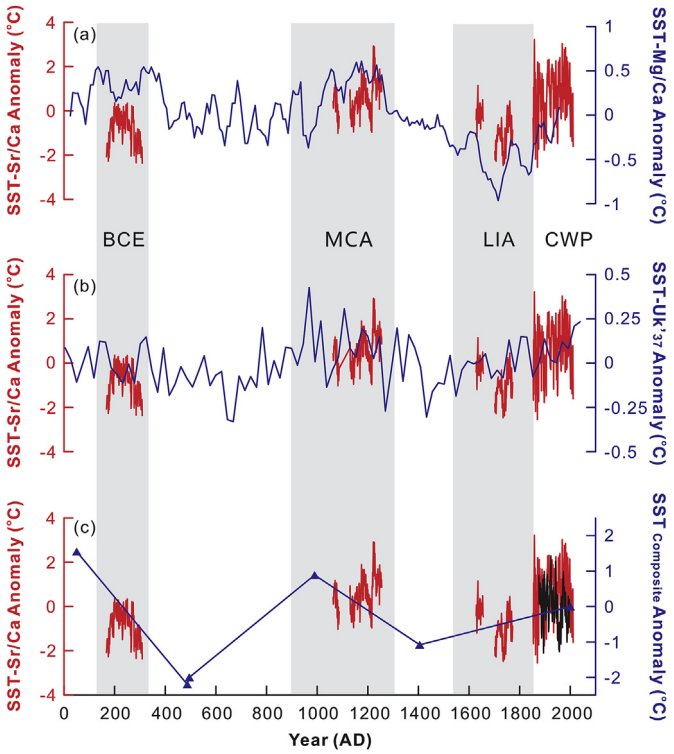

Fig. 5. Comparison of SST records based on coral Sr/Ca time series from the northern SCS (red lines) with the (a) SST records from composite foraminiferal Mg/Ca ratios in the Makassar Strait, Indonesia (Oppo et al., 2009), (b) SST records from the long-chain alkenones Uk'37 (Kong et al., 2017) (blue lines) and (c) composite SST records from coral and *Tridacna gigas* in the SCS (Yan et al., 2015a) (blue triangles), and SST record based on the Sr/Ca in another modern northern SCS coral (Liu et al., 2013) (black lines, sharing common y axis with the data of this study). The gray shading delineates the different periods. (For interpretation of the references to colour in this figure legend, the reader is referred to the Web version of this article.)

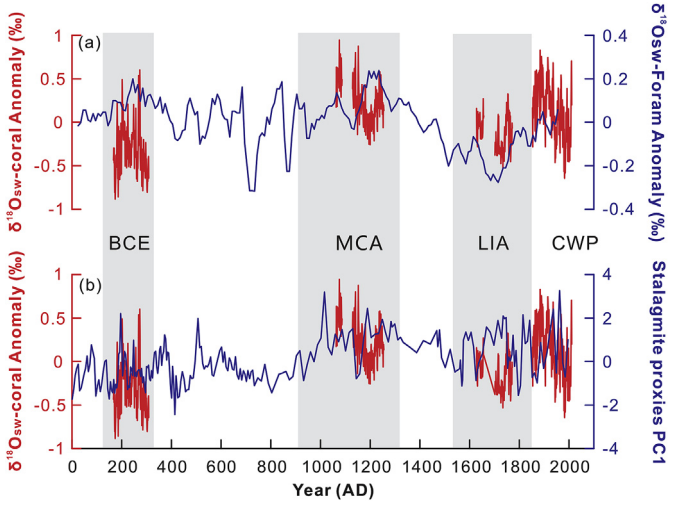

Fig. 6. Comparison of $\delta^{18}O_{sw}$ records based on coral Sr/Ca and $\delta^{18}O$ time series from the northern SCS (red lines) with the (a) $\delta^{18}O_{sw}$ records reconstructed from foraminiferal Mg/Ca and $\delta^{18}O$ profiles in multi-cores from the Makassar Strait, Indonesia (Oppo et al., 2009) and (b) leading principal component of stalagmite $\delta^{18}O$, Sr/Ca, and Mg/Ca from the eastern Indonesian island of Flores (Griffiths et al., 2016) (blue lines). The gray shading delineates the different periods. (For interpretation of the references to colour in this figure legend, the reader is referred to the Web version of this article.)

geochemical proxies in the western Pacific over the past 2000 years (Griffiths et al., 2016). This finding suggests that there has been a consistent low frequency oscillation in the western Pacific hydroclimate over the past 2000 years, which may be associated with the spatial variation of intertropical convergence zone and Pacific Walker Circulation (Yan et al., 2011; Griffiths et al., 2016). Even so, the decadal–interdecadal variabilities of $\delta^{18}O_{sw}$ have nuanced differences during different periods. The 20 yr periodicity appears in both the BCE and the CWP, but the 12 yr periodicity appears in MCA only. As for the 2–6 yr interannual periodicities of EASM or ENSO, given the low resolution (i.e., 5–15 yr) of the stalagmite records, high frequency oscillations such as ENSO-like variability cannot be captured.

Overall, the $\delta^{18}O_{sw}$, like the situation in SST variability, also shows much higher variation amplitude in the CWP than in the MCA, although the high averages of annual SST during these two periods are similar. This high variation amplitude in $\delta^{18}O_{sw}$ during the CWP should be the response of ocean hydrological cycle to intensified surface warming (Durack et al., 2012). In contrast the BCE resembles the CWP in terms of $\delta^{18}O_{sw}$ variability since they have similar variation amplitudes and similar oscillation periodicities (Table 2, Fig. 4e and h). However, both SST and its variation amplitude are much higher in the CWP than in the BCE. Different from other periods, the LIA stands out at the lowest variation amplitude and with the absence of low frequency oscillation in $\delta^{18}O_{sw}$, which may due to the low solar activity. The period AD 1628–1740 with lower $\delta^{18}O_{sw}$ variation amplitudes during the LIA agrees with the timing of Maunder minimum (AD 1645–1715), during which sunspots became exceedingly rare (Usoskin et al., 2015).

Although the $\delta^{18}O_{sw}$ variabilities are somewhat complicated, high variability during the CWP may still suggest the anthropogenic effects on the tropical oceanic hydroclimate. It has been suggested that intensified ocean hydrological cycle and salinity changes during AD 1955–2004 are inconsistent with natural causes but associated with anthropogenically-induced changes in greenhouse gases and aerosols (Pierce et al., 2012).

4.3. Anthropogenic effects on the climate change and carbon cycle in the SCS

The ocean had absorbed more than 93% of the excess heat from greenhouse gas emissions since 1970s, which is causing ocean temperatures to rise (IPCC, 2013). Simultaneous increases in the SST and the concentration of atmospheric CO_2 are also observed during the CWP in the present study; however, the increase in SST does not exhibit a linear response to the increase in the atmospheric CO_2 concentration (Fig. 7a). Therefore, the warmer SSTs during the CWP may partly due to elevated atmospheric CO_2 concentrations. The increase in SST during the CWP could also be partly due to the increase in total solar insolation (TSI, Fig. 7b) because SST peaks during the warmer MCA and colder LIA in the SCS coincide with increased and decreased TSI, respectively (Deng et al., 2017b). However, comparisons of the amplitude and frequency variability in SST between the human-influenced CWP and the BCE, MCA, and LIA that were controlled by natural forcings reveal a wider range and higher frequency variability in SST during the CWP than during the earlier periods. Therefore, human activities may be one of the drivers of more frequent extreme climate events in recent times (e.g., Mann et al., 2017).

The anthropogenic release of CO_2 depleted in ^{13}C through the burning of fossil fuels and deforestation has led to a decline in $\delta^{13}C$ levels in atmospheric CO_2 (Keeling, 1979; Friedli et al., 1986) and the oceanic $\delta^{13}C$ Suess effect (Böhm et al., 1996). The oceanic ^{13}C Suess effect has driven the decoupling of coral $\delta^{13}C$ and TSI at centennial-

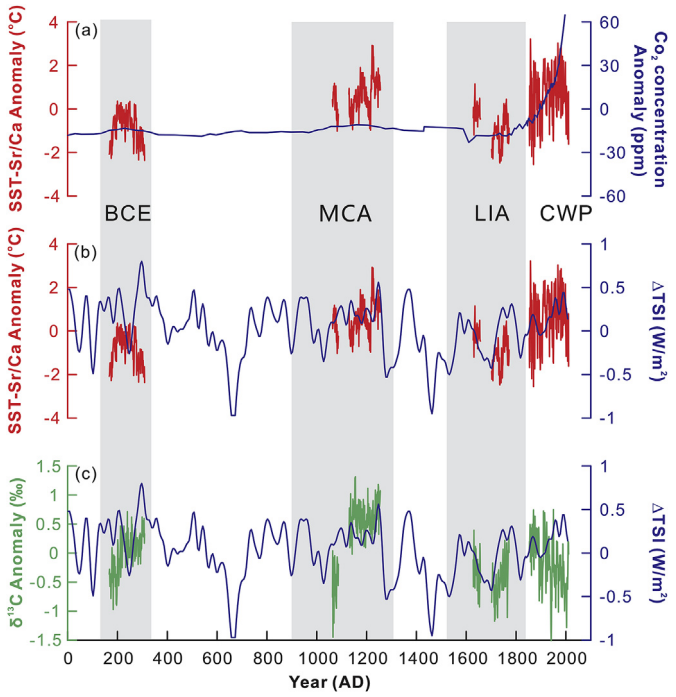

Fig. 7. Comparison of SST records based on coral Sr/Ca time series from the northern SCS (red lines) with the (a) atmospheric CO_2 concentration reconstructed from ice cores in Law Dome, Antarctica (MacFarling Meure et al., 2006) and (b) TSI reconstruction based on a recently observationally derived relationship between TSI and the open solar magnetic field (Steinhilber et al., 2009) (blue lines). (c) Comparison of coral $\delta^{13}C$ (red line) with the TSI reconstruction (Steinhilber et al., 2009) (blue line). The gray shading delineates the different periods. (For interpretation of the references to colour in this figure legend, the reader is referred to the Web version of this article.)

scale since the Industrial Revolution (Fig. 7c) (Deng et al., 2017a). This decoupling implies that the main carbon source and the utilization process of coral reefs during calcification have changed. During the earlier periods (i.e., BCE, MCA, and LIA) in which climatic changes were controlled by natural forcings, corals presumably utilized oceanic carbon reservoirs for building reefs and TSI controlled coral $\delta^{13}C$ levels by affecting the photosynthetic activity of the endosymbiotic zooxanthellae at the centennial scale. However, during the CWP, in which climatic changes are dominated by anthropogenic factors, more anthropogenic CO_2 is utilized during calcification. Therefore, anthropogenic CO_2 has undoubtedly had a significant effect on the surface ocean carbon cycle. This effect may subsequently feedback to other processes of the climate and environmental change, such as ocean acidification, at longer time scales. Therefore, the effects of anthropogenic CO_2 on oceanic climate and environmental change should be monitored continuously over a longer time frame.

5. Conclusions

Based on the synthesis and reanalysis of existing coral-based paleoclimate data from the northern SCS over the past 2000 years, the climatic changes and variabilities in SST and $\delta^{18}O_{sw}$ records during different climate periods were compared to assess anthropogenic effects on tropical oceanic climate change and variability. The main conclusions are as follows.

1. Compared with climate periods driven by natural forcings, the large anomaly range and high frequency variability in the SST records during the CWP suggests that anthropogenic effects intensify the tropical SST variability both in amplitude and frequency.
2. Despite similar interannual variabilites in $\delta^{18}O_{sw}$ during the CWP and climate periods controlled by natural forcings, high variability during the CWP may still suggest the anthropogenic effects on the tropical oceanic hydrological conditions.
3. Anthropogenic CO_2 has caused the main carbon source and utilization process of coral reefs during calcification to change.
4. The effects of anthropogenic CO_2 on oceanic climate and environmental change should be monitored continuously over a longer time frame.

Acknowledgments

The authors would like to thank the editor Henning Bauch and two anonymous reviewers for their helpful comments and constructive suggestions. Yi Liu is appreciated for kindly providing the coral Sr/Ca data. The English of the manuscript was improved by Stallard Scientific Editing. This work was supported by the National Key Research and Development Project of China (2016YFA0601204), the National Natural Science Foundation of China (41673115, 41722301) and the State Key Laboratory of Isotope Geochemistry (SKLIG-RC-14-02). This is contribution IS-2632 from GIGCAS. The data for this paper are available as the online supplementary data in Dataset S1.

Appendix A. Supplementary data

Supplementary data to this article can be found online at https://doi.org/10.1016/j.quascirev.2018.12.027.

References

Abram, N.J., Gagan, M.K., Cole, J.E., Hantoro, W.S., Mudelsee, M., 2008. Recent intensification of tropical climate variability in the Indian Ocean. Nat. Geosci. 1, 849–853.
Abram, N.J., McGregor, H.V., Gagan, M.K., Hantoro, W.S., Suwargadi, B.W., 2009. Oscillations in the southern extent of the indo-pacific warm pool during the mid-holocene. Quat. Sci. Rev. 28, 2794–2803.
Abram, N.J., McGregor, H.V., Tierney, J.E., Evans, M.N., McKay, N.P., Kaufman, D.S., the, P.k.C., Thirumalai, K., Martrat, B., Goosse, H., Phipps, S.J., Steig, E.J., Kilbourne, K.H., Saenger, C.P., Zinke, J., Leduc, G., Addison, J.A., Mortyn, P.G., Seidenkrantz, M.-S., Sicre, M.-A., Selvaraj, K., Filipsson, H.L., Neukom, R., Gergis, J., Curran, M.A.J., Gunten, L.v., 2016. Early onset of industrial-era warming across the oceans and continents. Nature 536, 411–418.
Alpert, A.E., Cohen, A.L., Oppo, D.W., DeCarlo, T.M., Gove, J.M., Young, C.W., 2016. Comparison of equatorial Pacific sea surface temperature variability and trends with Sr/Ca records from multiple corals. Paleoceanography 31, 252–265.
Böhm, F., Joachimski, M.M., Lehnert, H., Morgenroth, G., Kretschmer, W., Vacelet, J., Dullo, W.C., 1996. Carbon isotope records from extant Caribbean and South Pacific sponges: evolution of $\delta^{13}C$ in surface water DIC. Earth Planet. Sci. Lett. 139, 291–303.
Bradley, R.S., Jones, P.D., 1993. 'Little Ice Age' summer temperature variations: their nature and relevance to recent global warming trends. Holocene 3, 367–376.
Chen, X., Wei, G., Deng, W., Liu, Y., Sun, Y., Zeng, T., Xie, L., 2015. Decadal variations in trace metal concentrations on a coral reef: evidence from a 159 year record of Mn, Cu, and V in a Porites coral from the northern South China Sea. J. Geophys. Res. Oceans 120, 405–416.
Ciais, P., Sabine, C., Bala, G., Bopp, L., Brovkin, V., Canadell, J., Chhabra, A., DeFries, R., Galloway, J., Heimann, M., Jones, C., Le Quéré, C., Myneni, R.B., Piao, S., Thornton, P., 2013. Carbon and other biogeochemical cycles. In: Stocker, T.F., Qin, D., Plattner, G.-K., Tignor, M., Allen, S.K., Boschung, J., Nauels, A., Xia, Y., Bex, V., Midgley, P.M. (Eds.), Climate Change 2013: the Physical Science Basis. Contribution of Working Group I to the Fifth Assessment Report of the Intergovernmental Panel on Climate Change. Cambridge University Press, Cambridge, United Kingdom and New York, NY, USA, pp. 465–570.
Crowley, T.J., Lowery, T.S., 2000. How warm was the medieval warm period? Ambio 29, 51–54.
Deng, W., Chen, X., Wei, G., Zeng, T., Zhao, J.-x., 2017a. Decoupling of coral skeletal $\delta^{13}C$ and solar irradiance over the past millennium caused by the oceanic Suess effect. Paleoceanography 32, 161–171.
Deng, W., Liu, X., Chen, X., Wei, G., Zeng, T., Xie, L., Zhao, J.-x., 2017b. A comparison of the climates of the medieval climate anomaly, Little ice age, and current warm period reconstructed using coral records from the northern South China sea. J. Geophys. Res. Oceans 122, 264–275.

Deng, W., Wei, G., Xie, L., Ke, T., Wang, Z., Zeng, T., Liu, Y., 2013. Variations in the pacific decadal oscillation since 1853 in a coral record from the northern South China sea. J. Geophys. Res. Oceans 118, 2358–2366.

Deng, W., Wei, G., 2014. Local origins of interdecadal Pacific variability in the tropical and North Pacific Ocean: evidence from a comparative study of coral oxygen isotope records. Geo Mar. Lett. 34, 345–352.

de Villiers, S., Shen, G.T., Nelson, B.K., 1994. The Sr/Ca-temperature relationship in coralline aragonite: influence of variability in $(Sr/Ca)_{seawater}$ and skeletal growth parameters. Geochem. Cosmochim. Acta 58, 197–208.

Durack, P.J., Wijffels, S.E., Matear, R.J., 2012. Ocean salinities reveal strong global water cycle intensification during 1950 to 2000. Science 336, 455–458.

Fleury, S., Martinez, P., Crosta, X., Charlier, K., Billy, I., Hanquiez, V., Blanz, T., Schneider, R.R., 2015. Pervasive multidecadal variations in productivity within the Peruvian Upwelling System over the last millennium. Quat. Sci. Rev. 125, 78–90.

Friedli, H., Lotscher, H., Oeschger, H., Siegenthaler, U., Stauffer, B., 1986. Ice core record of the $^{13}C/^{12}C$ ratio of atmospheric CO_2 in the past two centuries. Nature 324, 237–238.

Gagan, M.K., Ayliffe, L.K., Hopley, D., Cali, J.A., Mortimer, G.E., Chappell, J., McCulloch, M.T., Head, M.J., 1998. Temperature and surface-ocean water balance of the mid-Holocene tropical Western Pacific. Science 279, 1014–1018.

Gagan, M.K., Ayliffe, L.K., Beck, J.W., Cole, J.E., Druffel, E.R.M., Dunbar, R.B., Schrag, D.P., 2000. New views of tropical paleoclimates from corals. Quat. Sci. Rev. 19, 45–64.

Gagan, M.K., Dunbar, G.B., Suzuki, A., 2012. The effect of skeletal mass accumulation in *Porites* on coral Sr/Ca and $\delta^{18}O$ paleothermometry. Paleoceanography 27, PA1203. https://doi.org/10.1029/2011PA002215.

Ge, Q., Liu, H., Ma, X., Zheng, J., Hao, Z., 2017. Characteristics of temperature change in China over the last 2000 years and spatial patterns of dryness/wetness during cold and warm periods. Adv. Atmos. Sci. 34, 941–951.

Griffiths, M.L., Kimbrough, A.K., Gagan, M.K., Drysdale, R.N., Cole, J.E., Johnson, K.R., Zhao, J.-X., Cook, B.I., Hellstrom, J.C., Hantoro, W.S., 2016. Western Pacific hydroclimate linked to global climate variability over the past two millennia. Nat. Commun. 7, 11719.

Hammer, Ø., Harper, D.A.T., Ryan, P.D., 2001. PAST: Paleontological statistics software package for education and data analysis. Palaeontol. Electron. 4, 1–9.

Herr, D., Galland, G.R., 2009. The Ocean and Climate Change. Tools and Guidelines for Action. IUCN U.S. Multilateral Office, Gland, Switzerland.

IPCC, 2013. In: Stocker, T.F., Qin, D., Plattner, G.-K., Tignor, M., Allen, S.K., Boschung, J., Nauels, A., Xia, Y., Bex, V., Midgley, P.M. (Eds.), Climate Change 2013: the Physical Science Basis. Working Group I Contribution to the Fifth Assessment Report of the Intergovernmental Panel on Climate Change. Cambridge University Press, Cambridge, United Kingdom and New York, NY, USA, p. 282.

IPCC, 2014. In: Team, C.W., Pachauri, P.K., Meyer, L.A. (Eds.), Climate Change 2014: Synthesis Report. Contribution of Working Groups I, II and III to the Fifth Assessment Report of the Intergovernmental Panel on Climate Change, p. 151. Geneva, Switzerland.

Jing, Z.-y., Qi, Y.-q., Hua, Z.-l., Zhang, H., 2009. Numerical study on the summer upwelling system in the northern continental shelf of the South China Sea. Cont. Shelf Res. 29, 467–478.

Karl, T.R., Trenberth, K.E., 2003. Modern global climate change. Science 302, 1719–1723.

Keeling, C.D., 1979. The Suess effect: ^{13}Carbon-^{14}Carbon interrelations. Environ. Int. 2, 229–300.

Kellogg, W.W., 1977. Effects of Human Activities on Global Climate: a Summary, with Consideration of the Implications of a Possibly Warmer Earth. Technical Note. World Meteorological Organization.

Khandekar, M.L., Murty, T.S., Chittibabu, P., 2005. The global warming debate: a review of the state of science. Pure Appl. Geophys. 162, 1557–1586.

Kong, D., Wei, G., Chen, M.-T., Peng, S., Liu, Z., 2017. Northern South China Sea SST changes over the last two millennia and possible linkage with solar irradiance. Quat. Int. 459, 29–34.

Lamb, H.H., 1965. The early medieval warm epoch and its sequel. Paleogeogr. Paleoclimatol. Paleoecol. 1, 13–37.

Liu, Y., Peng, Z., Shen, C.-C., Zhou, R., Song, S., Shi, Z., Chen, T., Wei, G., DeLong, K.L., 2013. Recent 121-year variability of western boundary upwelling in the northern South China Sea. Geophys. Res. Lett. 40, 3180–3183.

Lough, J.M., 2010. Climate records from corals. Wiley Interdiscip. Rev.-Clim. Chang. 1, 318–331.

MacFarling Meure, C., Etheridge, D., Trudinger, C., Steele, P., Langenfelds, R., van Ommen, T., Smith, A., Elkins, J., 2006. Law Dome CO_2, CH_4 and N_2O ice core records extended to 2000 years BP. Geophys. Res. Lett. 33, L14810. https://doi.org/10.1029/2006GL026152.

Mann, M.E., 2002. The value of multiple proxies. Science 297, 1481–1482.

Mann, M.E., 2007. Climate over the past two Millennia. Annu. Rev. Earth Planet Sci. 35, 111–136.

Mann, M.E., Rahmstorf, S., Kornhuber, K., Steinman, B.A., Miller, S.K., Coumou, D., 2017. Influence of anthropogenic climate change on planetary wave resonance and extreme weather events. Sci. Rep. 7, 45242.

Mann, M.E., Zhang, Z., Hughes, M.K., Bradley, R.S., Miller, S.K., Rutherford, S., Ni, F., 2008. Proxy-based reconstructions of hemispheric and global surface temperature variations over the past two millennia. Proc. Natl. Acad. Sci. U. S. A 105, 13252–13257.

Masson-Delmotte, V., Schulz, M., Abe-Ouchi, A., Beer, J., Ganopolski, A., González Rouco, J.F., Jansen, E., Lambeck, K., Luterbacher, J., Naish, T., Osborn, T., Otto-Bliesner, B., Quinn, T., Ramesh, R., Rojas, M., Shao, X., Timmermann, A., 2013. Information from paleoclimate archives. In: Stocker, T.F., Qin, D., Plattner, G.-K., Tignor, M., Allen, K., Boschung, J., Nauels, A., Xia, Y., Bex, V., Midgley, P.M. (Eds.), Climate Change 2013: the Physical Science Basis. Contribution of Working Group I to the Fifth Assessment Report of the Intergovernmental Panel on Climate Change. Cambridge University Press, Cambridge, United Kingdom and New York, NY, USA, pp. 383–464.

McGregor, H.V., Dima, M., Fischer, H.W., Mulitza, S., 2007. Rapid 20th-Century increase in coastal upwelling off Northwest Africa. Science 315, 637–639.

McGregor, H.V., Evans, M.N., Goosse, H., Leduc, G., Martrat, B., Addison, J.A., Mortyn, P.G., Oppo, D.W., Seidenkrantz, M.-S., Sicre, M.-A., Phipps, S.J., Selvaraj, K., Thirumalai, K., Filipsson, H.L., Ersek, V., 2015. Robust global ocean cooling trend for the pre-industrial Common Era. Nat. Geosci. 8, 671–677.

Nurhati, I.S., Cobb, K.M., Lorenzo, E.D., 2011. Decadal-Scale SST and salinity variations in the central tropical Pacific: signatures of natural and anthropogenic climate change. J. Clim. 24, 3294–3308.

Okai, T., Suzuki, A., Kawahata, H., Terashima, S., Imai, N., 2002. Preparation of a new Geological Survey of Japan geochemical reference material: coral JCp-1. Geostand. Newsl. 26, 95–99.

Oppo, D.W., Rosenthal, Y., Linsley, B.K., 2009. 2,000-year-long temperature and hydrology reconstructions from the Indo-Pacific warm pool. Nature 460, 1113–1116.

Oreskes, N., 2004. The scientific consensus on climate change. Science 306, 1686-1686.

Pierce, D.W., Gleckler, P.J., Barnett, T.P., Santer, B.D., Durack, P.J., 2012. The fingerprint of human-induced changes in the ocean's salinity and temperature fields. Geophys. Res. Lett. 39, L21704. https://doi.org/10.1029/2012GL053389.

Pfeiffer, M., Dullo, W.-C., Zinke, J., Garbe-Schönberg, D., 2009. Three monthly coral Sr/Ca records from the Chagos Archipelago covering the period of 1950–1995 A.D.: reproducibility and implications for quantitative reconstructions of sea surface temperature variations. Int. J. Earth Sci. 98, 53–66.

Robock, A., 1979. The "Little ice age": northern hemisphere average observations and model calculations. Science 206, 1402–1404.

Song, S.H., Zhou, W.J., Peng, Z.C., Liu, W.G., Cheng, P., Xian, F., 2006. Response to environmental conditions of coral $\delta^{18}O$ of *Porites lutea* from shalao, hainan island. Mar. Geol. Quat. Geol. 26, 23–28 (in Chinese with English abstract).

Steinhilber, F., Beer, J., Fröhlich, C., 2009. Total solar irradiance during the Holocene. Geophys. Res. Lett. 36, L19704. https://doi.org/10.1029/2009GL040142.

Usoskin, I.G., Arlt, R., Asvestari, E., Hawkins, E., Käpylä, M., Kovaltsov, G.A., Krivova, N., Lockwood, M., Mursula, K., O'Reilly, J., Owens, M., Scott, C.J., Sokoloff, D.D., Solanki, S.K., Soon, W., Vaquero, J.M., 2015. The Maunder minimum (1645–1715) was indeed a grand minimum: a reassessment of multiple datasets. Astron. Astrophys. 581, A95. https://doi.org/10.1051/0004-6361/201526652.

Wang, B., LinHo Zhang, Y., Lu, M.-M., 2004. Definition of South China sea monsoon onset and commencement of the east asia summer monsoon. J. Clim. 17, 699–710.

Wang, C., Wang, W., Wang, D., Wang, Q., 2006. Interannual variability of the South China sea associated with El Niño. J. Geophys. Res. Oceans 111, C03023. https://doi.org/10.1029/2005JC003333.

Wei, G., Wang, Z., Ke, T., Liu, Y., Deng, W., Chen, X., Xu, J., Zeng, T., Xie, L., 2015. Decadal variability in seawater pH in the West Pacific: evidence from coral $\delta^{11}B$ records. J. Geophys. Res. Oceans 120, 7166–7181.

Wu, W., Tan, W., Zhou, L., Yang, H., Xu, Y., 2012. Sea surface temperature variability in southern Okinawa Trough during last 2700 years. Geophys. Res. Lett. 39, L14705. https://doi.org/10.1029/2012GL052749.

Xiao, H., Deng, W., Chen, X., Wei, G., Zeng, T., Zhao, J.-x., 2017. Wet and cold climate conditions recorded by coral geochemical proxies during the beginning of the first millennium CE in the northern South China Sea. J. Asian Earth Sci. 135, 25–34.

Yan, H., Sun, L., Oppo, D.W., Wang, Y., Liu, Z., Xie, Z., Liu, X., Cheng, W., 2011. South China Sea hydrological changes and Pacific Walker Circulation variations over the last millennium. Nat. Commun. 2, 293.

Yan, H., Soon, W., Wang, Y., 2015a. A composite sea surface temperature record of the northern South China Sea for the past 2500years: a unique look into seasonality and seasonal climate changes during warm and cold periods. Earth Sci. Rev. 141, 122–135.

Yan, H., Wei, W., Soon, W., An, Z., Zhou, W., Liu, Z., Wang, Y., Carter, R.M., 2015b. Dynamics of the intertropical convergence zone over the western pacific during the Little ice age. Nat. Geosci. 8, 315–320.

Zinke, J., Reuning, L., Pfeiffer, M., Wassenburg, J.A., Hardman, E., Jhangeer-Khan, R., Davies, G.R., Ng, C.K.C., Kroon, D., 2016. A sea surface temperature reconstruction for the southern Indian Ocean trade wind belt from corals in Rodrigues Island (19° S, 63° E). Biogeosciences 13, 5827–5847.